Available online at www.sciencedirect.com
ScienceDirect
Polymer 49 (2008) 422–431
polymer
www.elsevier.com/locate/polymer

Synthesis and thermal properties of telechelic poly(lactic acid) ionomers

Andrew J. Ro [a], Samuel J. Huang [a,b], R.A. Weiss [a,c,*]

[a] Polymer Program, University of Connecticut, 97 N. Eagleville Road, Storrs, CT 06269-3136, USA
[b] Department of Chemistry, University of Connecticut, 97 N. Eagleville Road, Storrs, CT 06269-3136, USA
[c] Department of Chemical Engineering, University of Connecticut, 97 N. Eagleville Road, Storrs, CT 06269-3136, USA

Received 19 August 2007; received in revised form 7 November 2007; accepted 17 November 2007
Available online 21 November 2007

Abstract

Telechelic poly(lactic acid) (PLA) ionomers were synthesized using a chemical recycling process. A transesterification reaction between a commercial PLA and 2-hydroxyethyl methacrylate or ethylene glycol was used to produce a hydroxy-terminated PLA. The hydroxy-terminated PLA was then reacted with itaconic anhydride to produce terminal carboxylic acid groups, which were neutralized with appropriate metal acetates to produce Na-, Li-, K-, Zn-, Ca- and Y-ω- and α,ω-telechelic PLA ionomers. ^{1}H NMR spectroscopy was used to confirm the presence of the itaconic acid end-groups and FTIR spectroscopy was used to quantify the extent of neutralization. The addition of the ionic groups increased the glass transition (T_g), and T_g increased as the strength of the ion-pair increased. The ionic groups suppressed crystallinity, especially when multivalent cations were used.

Keywords: Poly(lactic acid); Ionomers; Synthesis

1. Introduction

Petroleum-based polymers are not easily recyclable and do not biodegrade, which presents significant problems in waste management [1]. In 2003, the United States generated 26.7 million tons of plastic waste, of which only 5.2% was recycled [2]. In addition, the increasing price of petroleum has led to corresponding increases in monomer costs [3]. One alternative to petroleum-based polymers is renewable, plant-based polymers, such as poly(lactic acid) (PLA). PLA has thermal and mechanical properties similar to current commodity polymers but there is considerable interest in improving its glass transition temperature (T_g), melt processibility, toughness, and compatibility with other polymers [4–6].

Attempts to improve the properties of PLA have included orientation of the polymer [7], blending it with other biodegradable polymers [8], and copolymerization [9]. Integration of ionic groups on the polymer chain is another approach for improving the properties of polymers [10]. Ionomers typically contain a small amount (e.g., ≤15 mol%) of bonded salt groups. The majority of investigations of these materials consider random ionomers, where the ionic groups are randomly distributed on the polymer chain [11]. However, telechelic ionomers are generally used as model systems for understanding ionic aggregation behavior and morphology [12]. Telechelic ionomers are ideal for these investigations since the molecular weight between the ionic groups is controlled and the ionic groups are located exclusively at the ends of the polymer chain.

The improvements in thermal and mechanical properties of ionomers are attributed to nanophase separation of the ionic species, which forms due to strong ion–dipole interactions between the bonded salt groups. The interactions between the ionic groups act as reversible crosslinks, providing physical characteristics of a crosslinked polymer, but processibility is possible in solution or in the melt at elevated temperatures

* Corresponding author. Department of Chemical Engineering, University of Connecticut, 97 N. Eagleville Road, Storrs, CT 06269-3136, USA. Tel.: +1 860 486 4698; fax: +1 860 486 6048.
E-mail address: rweiss@mail.ims.uconn.edu (R.A. Weiss).

0032-3861/$ - see front matter © 2007 Elsevier Ltd. All rights reserved.
doi:10.1016/j.polymer.2007.11.038

[10]. The ionic groups restrict the segmental mobility of the polymer chain, which increases the T_g of the polymers [13,14]. In his early theoretical work, Eisenberg proposed that the extent of the increase should be dependent on the concentration and strength of the ion-pair interactions, specifically cq/a, where q is the cation charge, a is the ionic radius of the counter-ion and c is the ion concentration [15].

Sherman and Storey [16] previously synthesized telechelic PLA carboxylate ionomers and demonstrated that the presence of the metal carboxylates increased T_g and hindered crystallization. In the current study, ω- and α,ω-carboxylic acid-functional PLAs were synthesized by a chemical recycling process [17] using polymers and monomers derived from renewable resources. An alcoholysis reaction between itaconic anhydride and hydroxy groups produces carboxylic acid moieties. The chemical recycling process is a transesterification reaction between high molecular weight PLA and a hydroxy-terminated monomer and a subsequent end-capping reaction with itaconic anhydride. Itaconic anhydride is produced from the pyrolysis of citric acid or the fermentation of carbohydrates (both of which are renewable resources), followed by dehydration [18]. A reaction similar to the chemical recycling reaction is to use amines instead of hydroxy groups [19,20]. The functionalized PLA was neutralized with metal acetates of various valencies (Na^+, Li^+, K^+, Ca^{+2}, Zn^{+2}, Y^{+3}). This paper describes the effect of the metal ion concentration, metal ion valency, and the location of the ionic moieties on the thermal and mechanical properties of the telechelic PLA ionomers.

2. Experimental

2.1. Materials

PLA with a $M_n = 65{,}000$ g/mol and $M_w = 121{,}000$ g/mol (as determined by gel permeation chromatography using polystyrene standards) was obtained from Cargill Corp. (now, Natureworks, LLC) and was dried in a vacuum oven at 70 °C under reduced pressure for 12 h. Chloroform (Aldrich Chemical Co., 99.5%) was distilled over calcium hydride prior to use. 2-Hydroxyethyl methacrylate (HEMA, Sigma Chemical Co., 97%) was distilled under reduced pressure. All other reagents were used without further purification. Tin(II) 2-ethylhexanoate (SnOct, ~95%), calcium acetate, and itaconic anhydride (95%) were purchased from Sigma Chemical Co. Ethylene glycol (EG, anhydrous, 99.8%) and yttrium(III) acetate hydrate were purchased from Aldrich Chemical Co. Methanol, tetrahydrofuran (99.9%), sodium acetate, and potassium acetate were purchased from Fisher Scientific Inc. Zinc acetate dihydrate and lithium acetate were purchased from Acros Organics Co.

2.2. Synthesis of ω-(carboxylic acid) PLA

All glasswares and the stir-blades were dried in an oven at 160 °C and allowed to cool over $CaSO_4$ in a desiccator prior to use. PLA was melted under a N_2 purge at 190 °C in a 250 mL flask equipped with a mechanical stirrer. SnOct (2% w/w PLA) and HEMA were injected into the reaction flask via syringe. HEMA was added in two different molar ratios (26 mol and 130 mol of lactic acid units in the PLA per mole of HEMA) to produce two different molecular weight polymers. The reaction mixture was heated and stirred at 190 °C for 2 h to reduce the molecular weight of the PLA and functionalize one end of it with HEMA, see Scheme 1(a) The reaction flask was then quenched in cold water and the HEMA-functionalized polymer was dissolved in chloroform. The reaction flask was purged with N_2 and a two-fold molar excess of itaconic anhydride (ITA) and SnOct (1% w/w PLA) was then added to the flask. A water-cooled condenser was attached to the flask and the end-capping reaction (Scheme 1(b)) was refluxed at 120 °C for 6 h. The polymers were precipitated with excess methanol, filtered, and dried at 70 °C in a vacuum oven for 24 h. Two different molecular weight telechelic PLAs were prepared, $M_n \sim 3.4$ kg/mol and $M_n \sim 13.0$ kg/mol. These polymers are denoted as HPLAx, where x is the number-average molecular weight determined by ^{1}H NMR (see Section 2.5 below).

2.3. Synthesis of α,ω-(carboxylic acid) PLA

The carboxylic acid functionalized α,ω-telechelic PLAs were prepared in a similar manner as the HPLAx polymers, except ethylene glycol (EG) was used instead of HEMA. Two different molar ratios of PLA and EG, 42:1 mol and 181:1 mol of lactic acid units in the PLA to mole EG, and 2% SnOct (w/w PLA) were used to produce two different molecular weights, see Scheme 2(a). For the end-capping reaction, a four-fold molar excess of ITA and 1% SnOct (w/w PLA) were added to the α,ω-hydroxy terminated PLA solution under N_2, see Scheme 2(b). A water-cooled condenser was added to the reaction flask and the end-capping reaction was refluxed at 120 °C for 12 h under N_2. The product was precipitated with excess methanol, filtered, and dried at 70 °C in a vacuum oven for 24 h. α,ω-Carboxylic acid telechelic

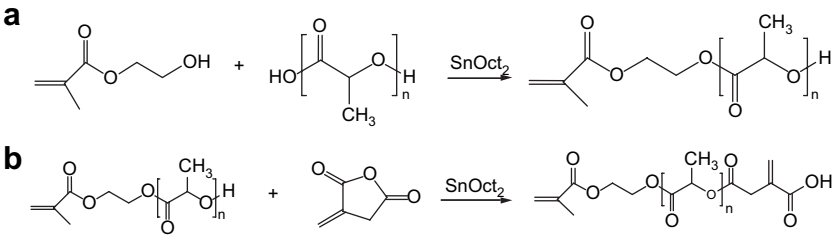

Scheme 1. (a) Synthesis of α-methacrylate-ω-hydroxy-PLA and (b) end-capping reaction with itaconic anhydride.

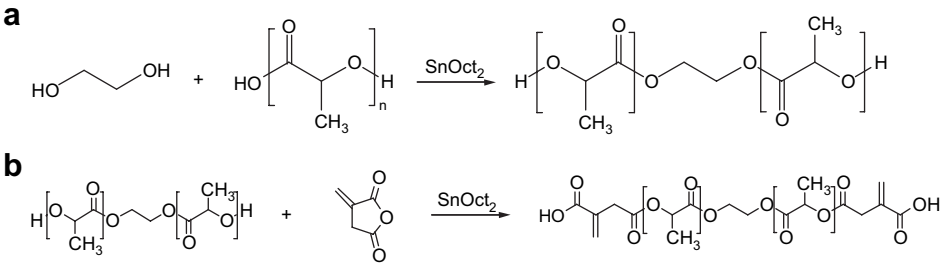

Scheme 2. (a) Synthesis of α,ω-(hydroxy) PLA and (b) end-capping reaction with itaconic anhydride.

polymers with $M_n \sim 3.4$ kg/mol and ~ 13.0 kg/mol (EPLA*x*, where $x = M_n$ from ^{1}H NMR) were prepared.

2.4. Preparation of ionomers

Stock solutions of the metal acetates (0.25 M) were prepared using distilled, deionized water. The HPLA*x* or EPLA*x* was dissolved in tetrahydrofuran (THF) in a round-bottom flask, and the following equivalents of metal acetate per equivalent of carboxylic acid were added to the reaction flask: 1 equiv for monovalent metal acetates, 2 equiv for divalent metal acetates, and 3 equiv for trivalent metal acetates. After allowing the neutralization reaction to proceed for 0.5 h, the solvent was vacuum distilled and the precipitated polymer was dried at 70 °C under reduced pressure for 24 h. The polymer was then washed with excess distilled, deionized water to remove any acetic acid and unreacted metal acetate, filtered, and dried at 70 °C under reduced pressure for 24 h. The sample nomenclatures for the telechelic ionomers are HPLA*x*–M and EPLA*x*–M, where M is the metal counter-ion (Na^+, Li^+, K^+, Ca^{+2}, Zn^{+2}, Y^{+3}).

2.5. Polymer characterization

FTIR spectra were measured with a Nicolet Magna IR 560 spectrometer using pellets prepared from KBr powder (Fisher Scientific Inc., 99.9%). Each sample was analyzed with 128 scans with 2 cm^{-1} resolution. ^{1}H NMR spectra were acquired on a Bruker DRX-500 MHz using 5 mm o.d. sample tubes. Samples were analyzed in $CDCl_3$ (Cambridge Isotope Laboratories, Inc.) containing 1% TMS as an internal reference. The number-average molecular weights (M_n) were determined by ^{1}H NMR from the ratio of the methine protons in the lactic acid repeat unit and the terminal vinyl protons.

The molecular weight averages M_n and M_w were also measured using a Waters 717 Plus autosampler gel permeation chromatography system equipped with a Waters 410 differential refractometer, a Waters 2487 dual wavelength absorbance UV–vis detector set at 254 nm, a Polymer Laboratories PL-ELS 1000 evaporative light scattering (ELS) detector, and a Jordi Gel DVB 105 Å, a PL Gel 10.4 nm, a Jordi Gel DVB 10 nm, and a Waters Ultrastyragel 50 nm column setup. Tetrahydrofuran (Fisher, 99.9% HPLC grade) was used as an eluent at a flow rate of 2 mL/min. Number-average (M_n) and weight-average molecular weights (M_w) were determined from calibration plots constructed with polystyrene standards.

Thermal properties were analyzed with a TA Instruments Q100 differential scanning calorimeter and samples were sealed in aluminum pans and experiments were run under an argon atmosphere. The sample thermal history was removed by heating the sample to 170 °C for 5 min and then quenching to −30 °C before all thermal analyses. The sample was heated from −30 °C to 170 °C, at a rate of 20 °C/min. Non-isothermal crystallization kinetic studies were conducted by heating the sample to 170 °C for 5 min and then cooling to −30 °C, at a rate of 5 °C/min. Temperatures and enthalpies were calibrated using an indium standard.

Thermomechanical analysis was conducted on a TA Instruments Q400 Thermomechanical Analyzer. A penetration probe with a force of 70 mN was applied to film sample that was 1.5–1.7 mm thick. The samples were heated from 10 °C to 140 °C at the rate of 10 °C/min. The ionomer samples were molded in a Teflon mold at 180 °C under reduced pressure in a vacuum oven.

3. Results and discussion

3.1. Structural characterization

^{1}H NMR spectroscopy was used to confirm the end-capping reactions of HPLA3.4 and HPLA13.0 and the spectra of HPLA3.4 and the intermediate HEMA terminated PLA are shown in Fig. 1. The methylene protons of HEMA, c and d, shifted down-field to a single broad peak at 4.35 ppm and the methylene protons of itaconic anhydride, h, shifted up-field to a broad peak at 3.42 ppm confirming the presence of the ITA and methacrylate end-groups. Integrations of the end-group protons indicated equimolar amounts of the two end-groups, which indicated that the functionalization reactions were quantitative and each chain had one carboxylic acid end-group and one methacrylate end-group (Table 1). The molar concentrations of itaconic acid end-groups in HPLA3.4 and HPLA13.0 were 2.2% and 0.6%, respectively.

Fig. 2 shows the ^{1}H NMR spectra of EPLA3.4 and its EG contained intermediate and its structural assignments. The singlet resonance at 4.30 ppm is due to the methylene protons, c, from the ethylene glycol, and the broad peak at 3.40 ppm is due to the methylene protons from the ITA end-groups, d. The integration ratio of the methylene protons, c, and the terminal vinyl protons, e and f, was used to verify the yield of the end-capping reaction (Table 1). The molar ratio of the ITA and the EG units was 2:1, which confirmed the presence of

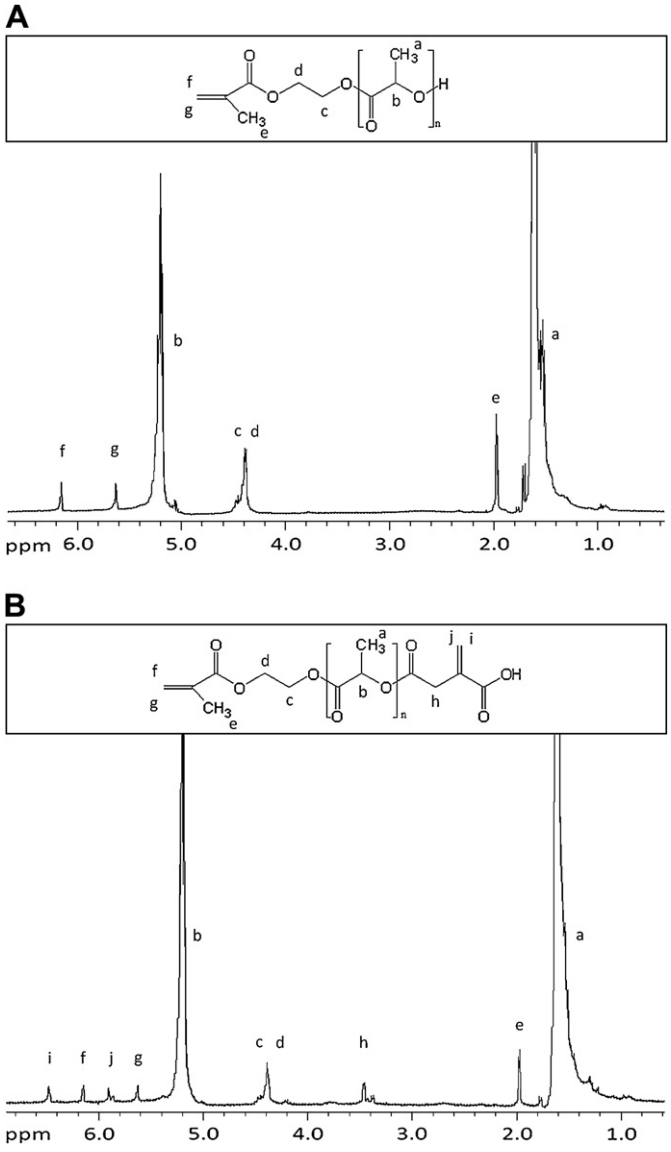

Fig. 1. ^{1}H NMR spectrum and structural assignments of HPLA3.4 before (A) and after (B) the end-capping reaction with itaconic anhydride. The integrations are summarized in Table 1.

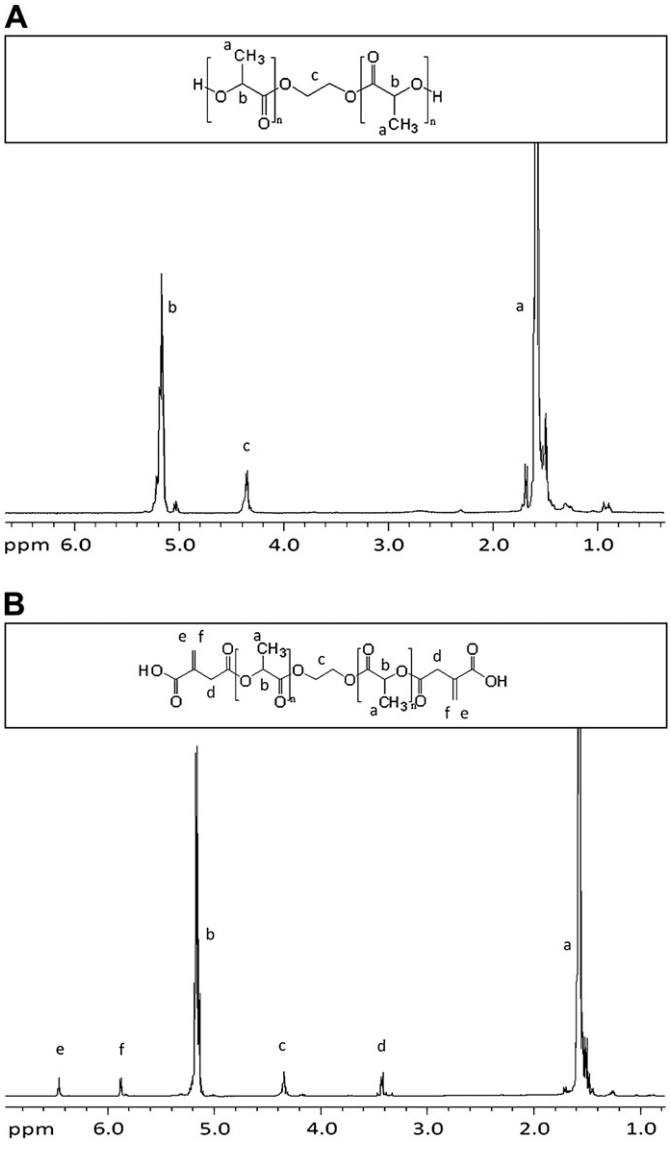

Fig. 2. ^{1}H NMR spectrum and structural assignments of EPLA3.4 before (A) and after (B) the end-capping reaction with itaconic anhydride. The integrations are summarized in Table 1.

Table 1
HPLA3.4 and EPLA3.4 samples: integrations from ^{1}H NMR spectra

Proton	HPLA3.4 (spectrum A)	HPLA3.4 (spectrum B)	EPLA3.4 (spectrum A)	EPLA3.4 (spectrum B)
a	120.0	120.2	33.0	68.9
b	39.7	43.3	10.9	22.9
c	4.0	4.0	1.0	2.2
d				1.9
e	2.9	3.2		1.0
f	1.0	0.9		1.0
g	1.1	1.0		
h		1.7		
i		1.0		
j		1.1		

itaconic acid end-groups at both ends of the PLA chain. The molar concentrations of itaconic acid end-groups in EPLA3.4 and EPLA8.9 were 4.5% and 1.7%, respectively.

Table 2 summarizes the molecular weights, thermal properties, and ion exchange capacity (IEC) of HPLA*x* and EPLA*x*. The IEC was calculated from the ratio of itaconic acid end-groups and lactic acid units determined from the NMR spectra. The molecular weights determined from end-group analysis (^{1}H NMR) coincided fairly well with the target molecular weights. The cause of these slight differences can be explained from the mechanism of the transesterification reaction. Kricheldorf et al. used detailed NMR experiments to show that SnOct initially reacts with any alcohol present, thus liberating octanoic acid, and Sn(II) becomes a catalytic site for esterification [21]. Esterification reactions can occur between the octanoic acid and the PLA chain or the alcohol, which produces octanoic end-groups. Trace amounts of these end-groups can be detected in the NMR spectra shown in Figs. 1 and 2, specifically in the 0.6–2.5 ppm region. However, it is difficult

Table 2
HPLA*x* and EPLA*x* samples: molecular weight and thermal properties

Sample	Target M_n (kg/mol)	M_n (^{1}H NMR) (kg/mol)	M_n (GPC) (kg/mol)	PDI (GPC), M_w/M_n	IEC (mequiv/g)	T_g (°C)	T_m (°C)	ΔH_m (J/g)
HPLA3.4	3.5	3.4	6.4	1.2	0.29	40	141	47
HPLA13.0	13.0	13.0	9.8	1.2	0.077	45	149	42
EPLA3.4	3.5	3.4	4.5	1.4	0.59	39	127	26
EPLA8.9	13.0	8.9	6.6	1.3	0.22	46	144	38

to quantify the amount of octanoic end-groups due to overlapping peaks. There was a disparity between the molecular weights determined from ^{1}H NMR and GPC, which may be a consequence of using polystyrene standards. For the remainder of the paper, the M_ns calculated by end-group analysis are used. Completion of the chemical recycling reaction was taken as when the GPC chromatographs exhibited only a single peak. During the reaction, prior to completion, the GPC traces showed a bimodal distribution of molecular weights. The products of the chemical recycling reaction had polydispersities (PDI) ranging from 1.2 to 1.4.

The formation of the ω- and α,ω-(carboxylic acid) PLA ionomers was confirmed by FTIR spectroscopy, which showed the conversion of the carboxylic acid end-groups to metal carboxylate. Fig. 3 shows the FTIR spectra of EPLA3.4 and its various metal carboxylate derivatives. The strong absorption at ~1760 cm^{-1} and a shoulder at ~1750 cm^{-1}, present in all the spectra, were due to the carbonyl stretching from the PLA repeat units and non-hydrogen bonded carboxylate end-groups [22]. Because the polymer was predominantly PLA and the carbonyl bands for PLA and the itaconic acid

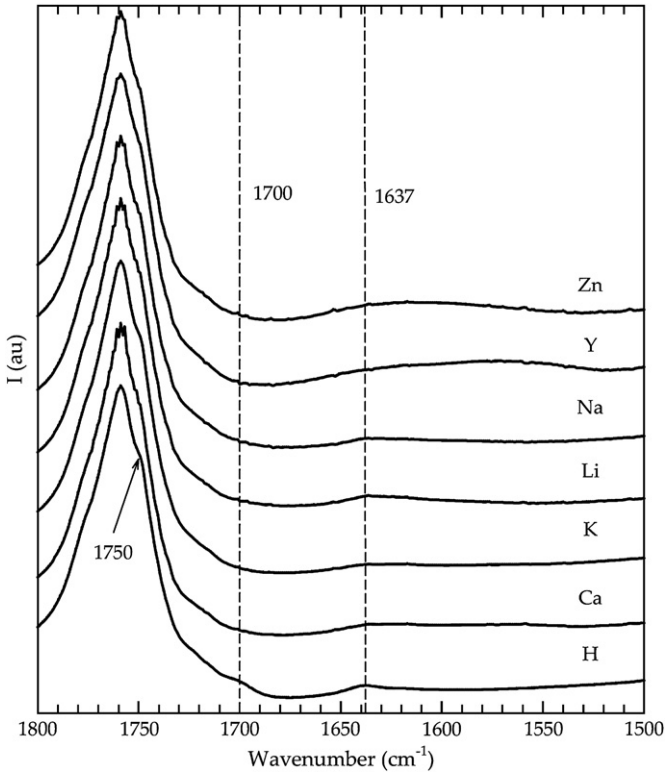

Fig. 3. FTIR spectra of EPLA3.4 and its various metal salts.

overlap, it was not possible to resolve that band into the contribution of the two components. A weak absorption at ~1700 cm^{-1} in the acid derivative was due to the carbonyl stretch in hydrogen bonded cyclic dimers of the carboxylic acids [23]. That band is absent in IR spectrum of PLA (not shown). The weak band at 1637 cm^{-1} is due to the vinyl groups in the ITA end-groups and it is present in all acid and the salt derivatives. Upon neutralization of the acid-terminated PLA, the absorption band at 1700 cm^{-1} disappears and the appearance of broad, weak band between 1500 cm^{-1} and 1650 cm^{-1} in the salts is consistent with the carbonyl stretching in the carboxylate anion. Because of the low concentration of ionic groups, the broadness of the carboxylate absorption and overlap of the vinyl absorption in the carbonyl region of the IR spectrum, quantitative analysis of the extent of neutralization of the ionomers was not possible. But the disappearance of the 1700 cm^{-1} band suggests that the neutralization level was either complete or, at least, relatively high.

3.2. Thermal analysis

3.2.1. Carboxylic acid derivatives

DSC heating thermograms for HPLA*x* and EPLA*x* samples quenched quickly from the melt are shown in Fig. 4. Each exhibited a T_g between 40 °C and 50 °C, which was followed by a cold crystallization exotherm that preceded the melting transition. The cold crystallization exotherms indicate that the quenched samples were not highly crystalline. Two melting endotherms were observed for each material. The lower temperature endotherm is probably associated with the melting of smaller crystallites formed during the quench procedure, and the higher temperature endotherm is due to the larger crystallites formed during cold crystallization as the sample was heated slowly during the heating cycle [24–26]. The melting temperature (T_m) was defined as the peak temperature of the highest temperature endotherm and the heat of fusion (ΔH_m) was determined from the integration of both endothermic peaks.

The thermal properties of the acid derivatives are summarized in Table 2. The T_gs of the polymers increased with increasing molecular weight, which is expected since the molecular weights were low and within the region where a decrease in the concentration of chain-ends (i.e., increasing molecular weight) increases T_g. There did not appear to be a significant effect of the number of carboxylic acid groups per chain (one or two) on T_g. For each type of telechelic polymer, the T_m increased with increasing molecular weight, which corresponded to decreasing carboxylic acid concentration. In general, the EPLA*x* had lower T_m and crystallinity (i.e., ΔH_m) decreased

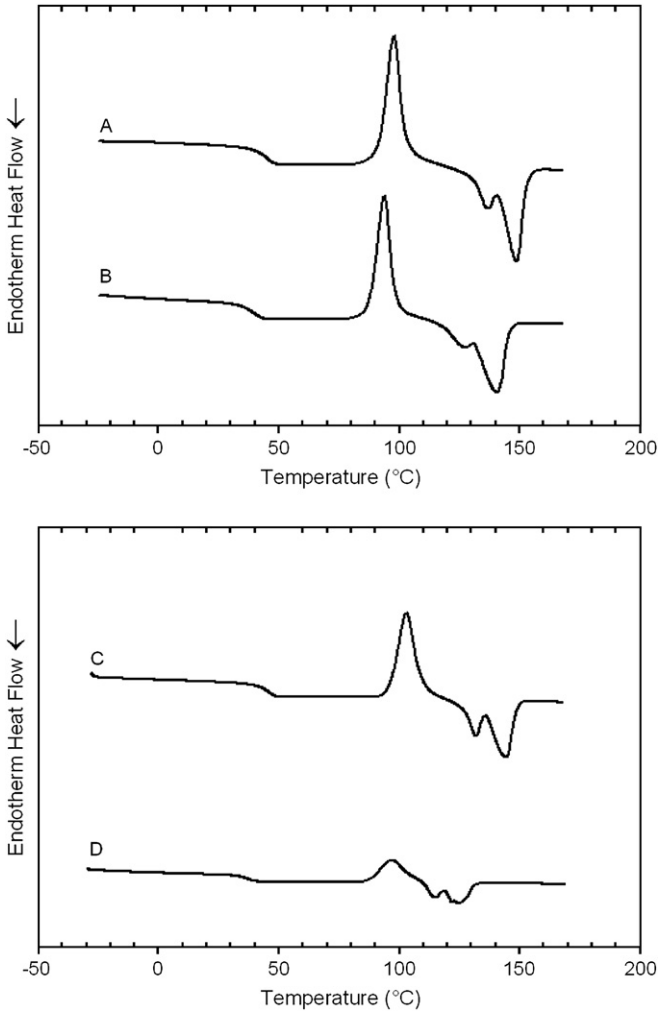

Fig. 4. DSC thermograms of (A) HPLA13.0, (B) HPLA3.4, (C) EPLA8.9, and (D) EPLA3.4. The heating rate was 20 °C/min following a rapid quench from 170 °C.

than HPLA*x* of comparable molecular weight, which would correspondingly have half the ionic concentration. Although it is not possible to completely separate the effects of molecular weight and acid concentration with these limited data, it does appear that the presence of the acid groups suppresses crystallinity and T_m of the polymers.

Non-isothermal crystallization studies (cooling at 5 °C/min from 170 °C) were used to assess the effect of the carboxylic end-groups on the crystallization kinetics of the telechelic PLAs. Typical cooling thermograms are shown in Fig. 5. The peak crystallization temperature (T_c), where the crystallization rate is a maximum, and the total enthalpy of crystallization (ΔH_c) under these conditions are summarized in Table 3. Fig. 6 compares the fractional crystallization (X_t) versus time for the HPLA*x* and EPLA*x* polymers. Fractional crystallization was defined as:

$$X_t = \frac{\Delta H_{c,T}}{\Delta H_c} \tag{1}$$

where $\Delta H_{c,T}$ is the heat of crystallization measured from the onset temperature for crystallization (T_o), see arrows in Fig. 5,

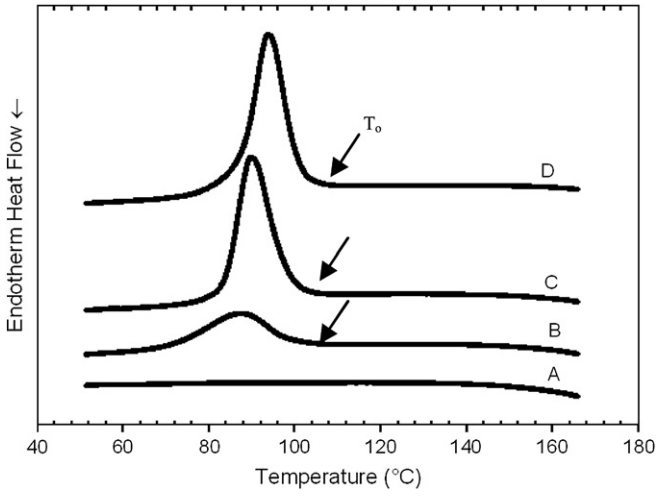

Fig. 5. DSC cooling thermograms for (A) EPLA3.4, (B) EPLA8.9, (C) HPLA3.4 and (D) HPLA13.0. The samples were cooled at 5 °C/min from 170 °C.

to an experimental temperature, T. The relationship between temperature T and time, t, is defined as:

$$t = \frac{|T_o - T|}{\Phi} \tag{2}$$

where Φ is the cooling rate (°C/min). Fractional crystallization data were linear with time and a crystallization rate constant,

Table 3
Summary of DSC results for HPLA*x*–M and EPLA*x*–M ionomers

Sample	IEC (mequiv/g)	*q*/*a*	T_m (°C)	ΔH_m (J/g)	T_c (°C)	ΔH_c (J/g)
HPLA13.0	0.077		149	42	96	36
HPLA13.0–K	0.077	0.72	153	46	100	42
HPLA13.0–Na	0.077	0.98	153	43	101	43
HPLA13.0–Li	0.077	1.7	152	45	102	45
HPLA13.0–Ca	0.077	2	154	48	111	46
HPLA13.0–Zn	0.077	2.4	153	44	111	46
HPLA13.0–Y	0.077	2.8	153	44	102	33
EPLA8.9	0.22		144	38	87	15
EPLA8.9–K	0.22	0.72	146	42	99	25
EPLA8.9–Na	0.22	0.98	145	41	90	36
EPLA8.9–Li	0.22	1.7	145	42	93	39
EPLA8.9–Ca	0.22	2	146	41	88	33
EPLA8.9–Zn	0.22	2.4	145	42	93	37
EPLA8.9–Y	0.22	2.8	141	28	89	13
HPLA3.4	0.29		141	47	91	32
HPLA3.4–K	0.29	0.72	144	43	105	48
HPLA3.4–Na	0.29	0.98	143	48	105	49
HPLA3.4–Li	0.29	1.7	144	44	104	44
HPLA3.4–Ca	0.29	2	145	44	107	44
HPLA3.4–Zn	0.29	2.4	144	35	90	22
HPLA3.4–Y	0.29	2.8	142	14	87	17
EPLA3.4	0.59		127	26	nc[a]	nc
EPLA3.4–K	0.59	0.72	129	29	86	24
EPLA3.4–Na	0.59	0.98	126	29	85	17
EPLA3.4–Li	0.59	1.7	127	33	84	29
EPLA3.4–Ca	0.59	2	128	11	82	6
EPLA3.4–Zn	0.59	2.4	128	6	83	3
EPLA3.4–Y	0.59	2.8	nc	nc	nc	nc

[a] nc = no crystallization.

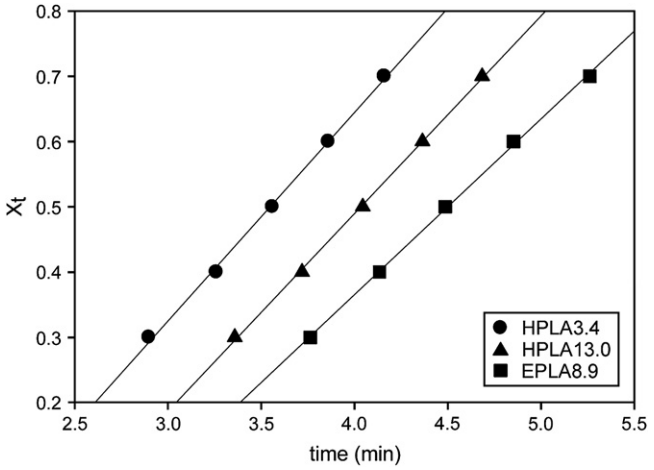

Fig. 6. Fractional crystallization versus time profiles for HPLAx and EPLAx ionomers calculated from non-isothermal crystallization studies.

α, was simply defined as the slope of the X_t versus time curve (i.e., $X_t \propto \alpha \cdot t$). The induction time for crystallization, t_i, as the sample was cooled from 170 °C was defined as:

$$t_i = \frac{|170 - T_o|}{\Phi} \tag{3}$$

The supercooling required for crystallization is the product Φt_i. The t_i and α calculations for the acid derivatives in Table 4 indicate that the induction time increased and the supercooling required for crystallization increased as the ion concentration (IEC) increased. That result is most likely a consequence of intermolecular hydrogen bonding occurring in these polymers, which suppresses molecular mobility.

3.2.2. Carboxylate ionomers

The T_gs of the ionomers are plotted as a function of q/a in Fig. 7. The T_gs of HPLAx–M and EPLAx–M ionomers were higher than the T_gs of their acid analogues, which is consistent with what is usually observed with ionomers [10] and the report by Sherman and Storey [16] that the T_g of a carboxylic acid-terminated PLA increased upon conversion to the Ca(II) salt. The higher T_g of the salts compared with the acid derivatives is due to the increased hindrance to segmental motion of the PLA chain as a result of interchain ion–dipole associations of the ionic groups, which are stronger than the hydrogen bonding in the acid derivatives. The increase of T_g for the ionomer is a consequence of the stronger ion–dipole interactions compared with hydrogen bonding, which further decreases molecular mobility. The increases in T_g shown in Fig. 7 appeared to be linearly dependent on q/a. Except for the EPLA3.4–M ionomers, the slope of the linear least squares fit of the data (the solid lines in Fig. 7) was similar, ~1.3–1.8 °C Å/charge. The 95% confidence limits of the linear fit are shown by dotted lines in Fig. 7. The different curves for each set of ionomers are due to the fact that for the low

Table 4
The induction time for non-isothermal crystallization (t_i) and rate of crystallization (α) of HPLAx–M and EPLAx–M ionomers (see text for definitions of t_i and α)

Counter-ion	q/a	t_i (s)			
		HPLA 13.0–M	EPLA 8.9–M	HPLA 3.4–M	EPLA 3.4–M
IEC (mequiv/g) →		0.077	0.22	0.29	0.59
H		10.5	12.2	11.8	
K	0.72	9.9	11.0	10.0	12.8
Na	0.98	9.7	10.8	10.4	13.3
Li	1.7	9.6	10.7	10.6	13.5
Ca	2.0	9.0	11.8	10.0	13.8
Zn	2.4	9.0	11.0	11.7	14.0
Y	2.8	9.2	11.0	11.9	nc[a]
		α ($\times 10^{-1}$)			
H		3.1	2.7	3.2	
K	0.72	3.9	2.6	4.4	2.6
Na	0.98	3.5	2.3	4.6	3.1
Li	1.7	3.6	3.4	4.6	3.7
Ca	2.0	5.3	3.0	5.1	2.6
Zn	2.4	5.0	3.7	2.8	2.7
Y	2.8	2.2	2.3	2.8	nc

[a] nc = no crystallization.

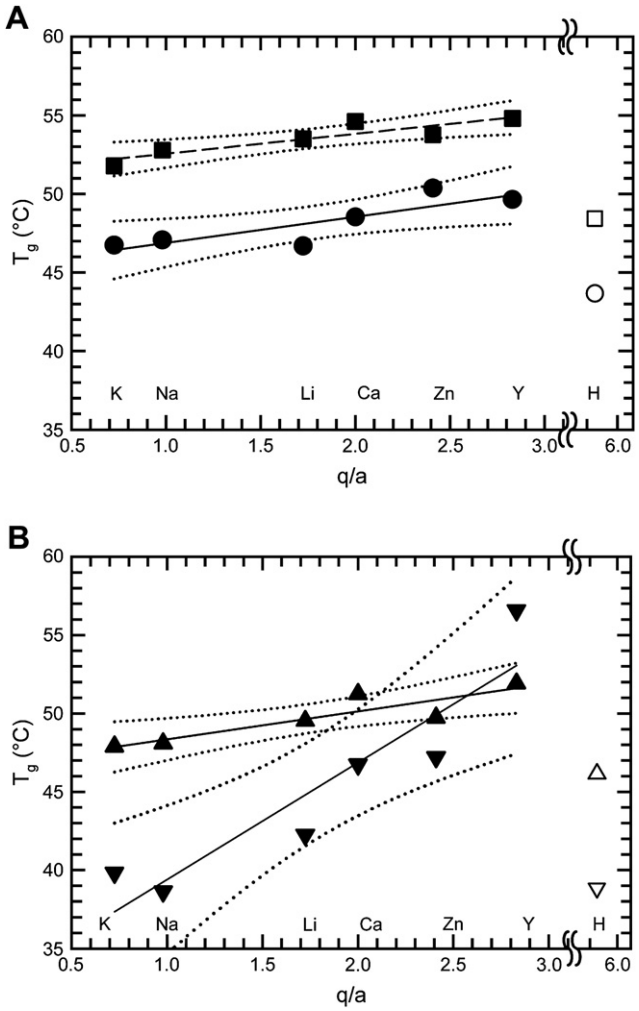

Fig. 7. T_g of the telechelic PLA ionomers as a function of q/a for (A) HPLAx and (B) EPLAx ionomers: (●) HPLA3.4; (■) HPLA13.0; (▼) EPLA3.4; (▲) EPLA8.9. The ionic radius, a, is defined in Å. The filled symbols are metal salts and the open symbols are the parent carboxylic acid derivatives. The solid lines are linear least square fits to the data and the dotted lines are the 95% confidence limits.

molecular weights used in this study, T_g is also dependent on molecular weight. Thus, the higher molecular weight ionomers exhibited higher absolute values for T_g, even though the effect of the ions on all the ionomers appeared to be similar.

The rate of the T_g increase of the EPLA3.4–M ionomers, which had the highest concentration of ionic groups, was about 4–5 times that of the other ionomers. The ionic concentrations in all of the materials studied were relatively low, and the greater effectiveness of the ion–dipole associations at increasing T_g in the EPLA3.4–M ionomers may be a consequence of the better network formation in that material, or perhaps a difference in the microstructure. SAXS measurements were made for the Y salts, which should have the greatest electron density contrast if nanophase separation of ionic aggregates occurred, but no "ionic peak" was observed for any of the samples. This may indicate that nanophase separation did not occur, but the failure to observe a peak in the SAXS data may simply be due to the very low concentration of the ionic species, which provides too little scattering contrast. The linear dependence of T_g on q/a indicates that the strength of the ion-pair controls the segmental mobility of the ionomer.

An attempt was made to develop a single T_g master curve by factoring in the concentration of ionic groups and the molecular weight of the polymer. Fig. 8 shows a plot of T_g of the ionomers normalized by the T_g or the acid derivative versus cMq/a, where $M = M_n$. The solid line is the linear least squares fit of all the data and the dotted curves represent the 95% confidence interval. Considering that there may be differences in the extent of neutralization of the different ionomer salts prepared (see earlier discussion on the uncertainty of the neutralization level), there does appear to be a correlation, may be even a linear relationship, between T_g and cq/a. However, more data are needed to confirm that conclusion.

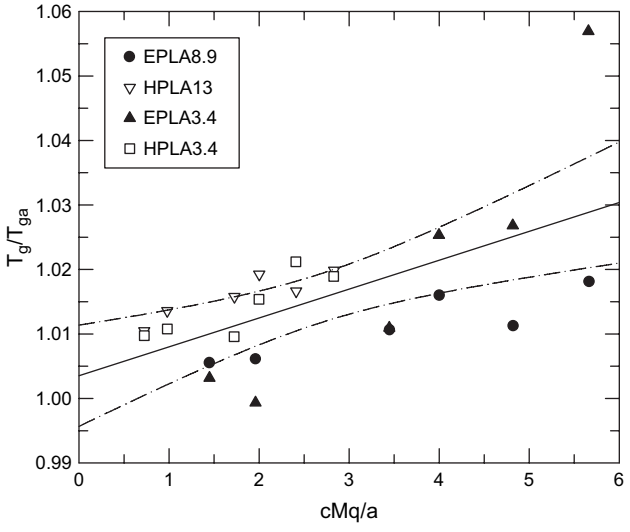

Fig. 8. T_g of the telechelic PLA ionomers normalized by the T_g of the parent acid-derivative (HPLAx or EPLAx) as a function of cMq/a: (●) HPLA3.4; (■) HPLA13.0; (▼) EPLA3.4; (▲) EPLA8.9. The concentration, c, is defined in mequiv/g and the ionic radius, a, is defined in Å. The solid lines are linear least squares fit to the data and the dotted lines are the 95% confidence limits.

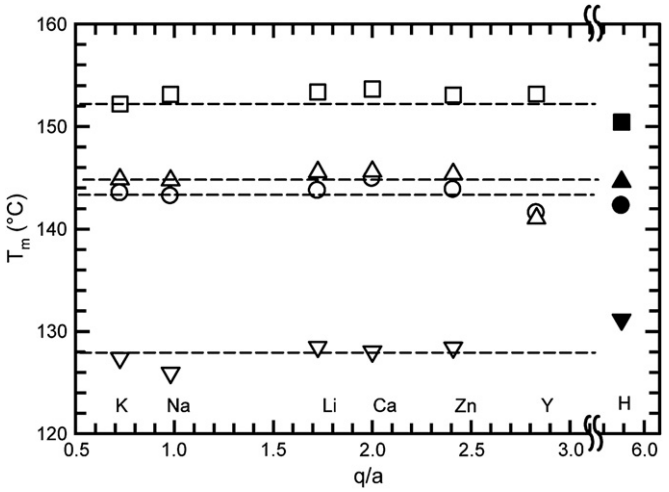

Fig. 9. Peak melting temperature of the telechelic PLA ionomers as a function of q/a for HPLAx and EPLAx ionomers: (○) HPLA3.4; (□) HPLA13.0; (▽) EPLA3.4; (△) EPLA8.9. The filled symbols denote the parent carboxylic acid derivatives. The ionic radius, a, is defined in Å.

Recent investigations [27–34] of the crystallization behavior of ionomers have addressed the effect of the ionic groups and nanophase separation of ionic aggregates in semi-crystalline ionomers. The ionic interactions in poly(ethylene-*co*-methacrylic acid) ionomers [27–30] and sulfonated syndiotactic polystyrene (SSPS) ionomers [31–33] decreased the rate of crystallization and suppressed crystallite growth. Nanophase separation in SSPS reduced the rate of crystallization, which was dependent on the counter-ion and the strength of the ionic interactions [30]. Moore and co-workers concluded that the strength of the electrostatic interactions of the different ions affected segmental motion, which governed the rate of the crystallization [31–33]. Ionic aggregation in poly(ethylene terephthalate) telechelic ionomers containing aromatic sulfonate end-groups also exhibited a decreased crystallization rate due to restricted polymer chain mobility from ionic interactions [34].

T_m, ΔH_m, T_c, and ΔH_c of the HPLAx–M and EPLAx–M ionomers were measured and calculated as described in the section concerning the carboxylic acid derivatives and are summarized in Table 3. T_m was relatively insensitive to the choice of the cation used in any of the ionomers (Fig. 9). There was some deviation for some of the acid derivatives and some of the Y salts from the average values of the other ionomers, but that may simply be due to some differences in the sample history, especially for the acid, which did not undergo the neutralization procedure. With the exception of the Zn(II) and Y(III) salts, ΔH_m also did not appear to vary with ionic concentration or cation (see Fig. 10). Crystallinity of the Zn(II) and Y(III) in the samples with the highest ion concentrations (EPLA3.4 and HPLA3.4) was significantly lower than that for the other salts and the EPLA3.4–Ca also had a very low crystallinity level. For the EPLA3.4–M, the Ca(II) and Zn(II) samples showed only traces of crystallinity and the Y(III) salt did not crystallize in the cooling experiment.

The values for t_i and α for the ionomers are summarized in Table 4. The data in Table 4 indicate that the induction time and the supercooling required for crystallization increased as

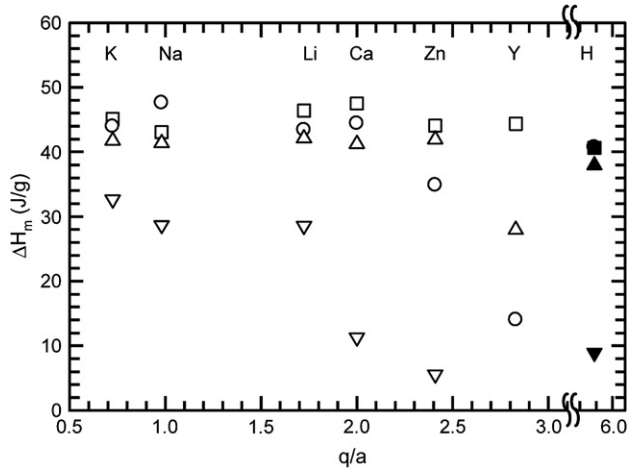

Fig. 10. Enthalpy of fusion of the telechelic PLA ionomers as a function of *q/a* for HPLA*x* and EPLA*x* ionomers: (○) HPLA3.4; (□) HPLA13.0; (▽) EPLA3.4; (△) EPLA8.9. The filled symbols denote the parent carboxylic acid derivatives. The ionic radius, *a*, is defined in Å.

the ionic concentration (IEC) increased and the strength of the ion-pair (*q/a*) increased. This is consistent with the idea that a reduction in the molecular mobility of the polymer melt was the primary influence on the onset of crystallization. The crystallization rate constant fluctuated for the different samples, but there did not appear to be any consistent trend of those data. Most likely, the fluctuations were due to the experimental errors in the X_t calculations, and to a first-approximation the rate was independent of the concentration of the ionic species and *q/a* of the cation. Similarly, no conclusions could be made for the effect of an ω-telechelic versus an α,ω-telechelic on the induction time.

3.3. Thermomechanical analysis

The TMA penetration profiles of HPLA3.4−M and EPLA3.4−M are shown in Fig. 11. The softening point of the polymer, which is related to the temperature dependence of the modulus, was similar for the acid derivatives and the alkali metal salts, but increased for the Ca(II), Zn(II) and Y(III) salts. The effect was most pronounced for the Y(III) salts. The other telechelic ionomers showed similar behavior, and the temperature values corresponding to 50% penetration, $T_{50\%}$, for all the ionomers are summarized in Table 5. In general, the softening point increased with the valency of the cation and ion concentration, which can be explained by the greater ease of forming a network with multivalent ions and higher concentration of the associating groups.

There are two types of interactions involving the ions that occur in ionomers. First, there is the formation of the ion-pair, and for multivalent cations, this can produce chain extension for divalent cations and network formation for trivalent and higher valency cations. In addition, there can be ion−dipole associations, as described earlier in this paper, that are responsible for ionic aggregation. The ionic aggregates also act as crosslinking sites in the formation of a physical network. With this in mind, it is not surprising that the trivalent, Y(III)

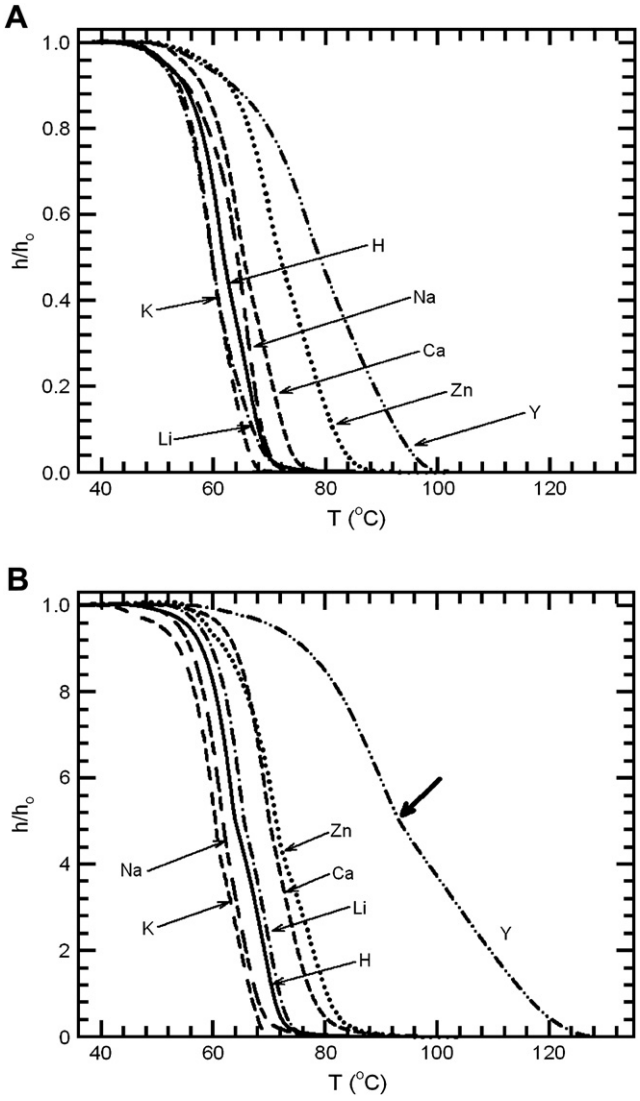

Fig. 11. TMA penetration curves for (A) HPLA3.4−M and (B) EPLA3.4−M. *h* is the height of the penetration probe and h_o is the height of the molded specimen. The dark arrow in part B denotes the inflection in the penetration behavior discussed in the text.

Table 5
Temperature corresponding to 50% TMA penetration for HPLA*x*−M and EPLA*x*−M ionomers ($T_{50\%}$)

Counter-ion	*q/a*	$T_{50\%}$ (°C)			
		HPLA 13.0−M	EPLA 8.9−M	HPLA 3.4−M	EPLA 3.4−M
IEC (mequiv/g) →		0.077	0.22	0.29	0.59
H		71.0	74.7	61.8	63.9
K	0.72	68.6	68.5	59.7	60.4
Na	0.98	69.4	69.8	64.3	61.8
Li	1.7	72.3	71.0	59.7	65.5
Ca	2.0	71.8	73.5	65.3	70.0
Zn	2.4	69.5	72.7	71.9	71.2
Y	2.8	78.7	79.1	78.9	93.2

cation provides the clearest indication of network formation in these telechelic ionomers. And, in the case of ion-dipole interactions involving divalent cations, the network functionality of the simplest physical case is four chains, while for the

monovalent cations, the simplest association of ion-pairs only provides chain extension. Thus, it is reasonable to expect that the divalent cations will more easily produce network characteristics than the monovalent cations.

Strong ion–dipole associations in ionomers often produce a sufficiently extensive physical network to produce a rubbery plateau in the viscoelastic behavior. Similar behavior has been previously observed by TMA for other ionomers, including telechelic ionomers [35]. Although no distinct ''plateau'' was observed for any of the telechelic ionomers, the EPLA3.4–M ionomers did exhibit an inflection in their penetration profiles, see Fig. 11B. This was most distinct in the Y(III) salt (see the dark arrow in Fig. 11B). Careful inspection of Fig. 11B reveals that the other EPLA3.4 salts, which had the highest ionic concentration of any of the telechelic ionomers studied, also exhibited an inflection in their TMA penetration curves. It is tempting to attribute this to something akin to molecular entanglements, which in this case would arise from strong, but transient associations of the ion-pairs. Unfortunately, the ionic concentration, is coupled inversely with the molecular weight of a telechelic polymer. Thus, to increase the ionic concentration to assess whether these materials can produce a more distinct rubbery region, is not very feasible since the molecular weight of EPLA3.4 was already very low.

4. Conclusions

A chemical recycling reaction is a facile way to prepare telechelic ionomers from PLA. The incorporation of neutralized carboxylic acid groups at the ends of a PLA chain increases the T_g of the polymer. The extent of the T_g change depends on the strength of the ion-pair, as measured by the ratio q/a, for metal carboxylates. Intermolecular ion–dipole interactions reduces molecular mobility and this suppressed the crystallization of the polymer. This effect was most noticeable for ionomers with multivalent cations, and in the case of a Y salt of a telechelic polymer containing 0.59 mequiv carboxylate/g, crystallinity was completely suppressed during a dynamic crystallization experiment, cooling from 170 °C at 5 °C/min. Although this work demonstrated the increases in T_g of PLA can be achieved by incorporating ionic groups into the polymer, in order to achieve reasonable levels of ion concentration with a telechelic polymer, the use of low molecular weight polymers is necessary. However, if similar results could be achieved by incorporating random ionic groups along the chain at levels of $\sim$1 mequiv/g, T_g increases by as much as 10 °C may be possible with multivalent cations. Even higher improvements in T_g would be expected for ion concentrations $>$ 1 mequiv/g.

Acknowledgments

This research was supported by the National Science Foundation (DMR-0328002).

References

[1] Huang SJ. J Macromol Sci Pure Appl Chem 1995;A32:593–7.
[2] Municipal solid waste generation, recycling, and disposal in the United States: facts and figures for 2003. U.S. Environmental Protection Agency; 2003.
[3] Tullo AH. Chem Eng News 2005;83:19–24.
[4] Sinclair RG. J Macromol Sci Pure Appl Chem 1996;A33(5):585–97.
[5] Lipinsky ES, Sinclair RG. Chem Eng Prog 1986;82:26–32.
[6] Mobley DP. Plastics from microbes: microbial synthesis of polymers and polymer precursors. Ohio: Hanser Gardner Publications; 1994.
[7] Grijpma DW, Altpeter H, Bevis MJ, Feijen J. Polym Int 2002;51(10): 845–51.
[8] Iannace S, Ambrosio L, Huang SJ, Nicolais L. J Appl Polym Sci 1994; 54:1525–35.
[9] Spinu M, Jackson C, Keating M, Gardner K. J Macromol Sci Pure Appl Chem 1996;A33(10):1497–530.
[10] Tant MR, Mauritz KA, Wilkes GL, editors. Ionomers: synthesis, structure, properties and applications. London, UK: Blackie Academic Press; 1997.
[11] Lantman CW, Macknight WJ. Annu Rev Mater Res 1989;19:295–317.
[12] Sobry R, Fontaine F, Ledent J, Foucart M, Jerome R. Macromolecules 1998;31:4240–52.
[13] Gao Zh, Zhong XF, Eisenberg A. Macromolecules 1994;27(2):794–802.
[14] Vanhoorne P, Jerome R, Teyssie P, Laupetre F. Macromolecules 1994;27:2548–52.
[15] Eisenberg A. Macromolecules 1971;4:125–8.
[16] Sherman JW, Storey RF. Polym Prepr (Am Chem Soc Div Polym Chem) 1999;40(2):952–3.
[17] Wallach JA, Huang SJ. ACS Symp Ser 2000;764:281–92.
[18] Larsen H, Eimhjellen KE. Biochem J 1955;60:135–9.
[19] Galanti AV, Scola DA. J Polym Sci Part A Polym Chem 1981;19: 451–75.
[20] Galanti AV, Keen BT, Pater RH, Scola DA. J Polym Sci Part A Polym Chem 1981;19:2243–53.
[21] Kricheldorf HR, Kreiser-Saunders I, Stricker A. Macromolecules 2000; 33:702–9.
[22] Kagarise RE. J Am Chem Soc 1955;77:1377–9.
[23] Lee YJ, Painter PC, Coleman MM. Macromolecules 1988;21:346–54.
[24] Wunderlich B. Macromolecular physics, vol. 3. New York: Academic; 1980.
[25] Yasuniwa M, Tsubakihara S, Sugimoto Y, Nakafuku C. J Polym Sci Part B Polym Phys 2003;42:25–32.
[26] Solarski S, Ferreira M, Devaux E. Polymer 2005;46:11187–92.
[27] Vanhoorne P, Register RA. Macromolecules 1996;29:598–604.
[28] McLean RS, Doyle M, Sauer BB. Macromolecules 2000;33:6541–50.
[29] Sauer BB, McLean RS. Macromolecules 2000;33:7939–49.
[30] Quiram DJ, Register RA, Ryan AJ. Macromolecules 1998;31:1432–5.
[31] Orler EB, Yontz DJ, Moore RB. Macromolecules 1993;26:5157–60.
[32] Orler EB, Moore RB. Macromolecules 1994;27:4774–80.
[33] Orler EB, Calhoun BH, Moore RB. Macromolecules 1996;29:5965–71.
[34] Hegedus RS, Long TE. Macromolecules 2002;35:8738–44.
[35] Bagrodia SR, Wilkes GL, Kennedy JP. J Appl Polym Sci 1985;30: 2179–93.